

# Ionic conductivity of the $\text{Na}_{1+x}\text{M}_x^{\text{III}}\text{Zr}_{2-x}(\text{PO}_4)_3$ systems (M = Al, Ga, Cr, Fe, Sc, In, Y, Yb)

J. M. WINAND, A. RULMONT, P. TARTE

*University of Liège, Institute of Chemistry, B-4000 Sart-Tilman par Liège, 1 Belgium*

The existence and ionic conductivity of solid solutions  $\text{Na}_{1+x}\text{M}_x^{\text{III}}\text{Zr}_{2-x}(\text{PO}_4)_3$  with Nasicon-like structure have been investigated and the results compared with literature data. A limited range of solid solutions is formed with  $\text{M}^{\text{III}}$  = aluminium, gallium, yttrium, ytterbium, whereas a continuous series is obtained for  $\text{M}^{\text{III}}$  = chromium, iron, scandium, indium. The pure end member  $\text{Na}_3\text{In}_2(\text{PO}_4)_3$  is reported for the first time; according to powder diffraction data, it is hexagonal with  $a = 0.8966(1)$  and  $c = 2.2104(4)$  nm. The small monoclinic distortion already known for  $\text{M}^{\text{III}}$  = chromium, iron and scandium is restricted to  $x$  values very close to 2. Ionic conductivity measurements show that for a given value of  $x$ , the mobility of the  $\text{Na}^+$  ions is strongly influenced both by the ionic radius and the type of electronic structure of the  $\text{M}^{\text{III}}$  ion. However, no simple correlation can be found.

## 1. Introduction

Since the discovery by Hong and co-workers [1, 2] of the ionic conductivity of the so-called Nasicon phase  $\text{Na}_3\text{Zr}_2\text{Si}_2\text{PO}_{12}$ , several papers have been devoted to the study of structurally related compounds such as  $\text{Na}_3\text{M}_2^{\text{III}}(\text{PO}_4)_3$  (M = Cr, Fe, Sc) [3-14] and solid solutions  $\text{Na}_{1+x}\text{M}_x^{\text{III}}\text{Zr}_{2-x}(\text{PO}_4)_3$  [15-17].

However, to the best of our knowledge, these studies have been restricted to medium-size  $\text{M}^{\text{III}}$  cations, and no attempt has been made to introduce, either smaller cations such as aluminium or gallium, or cations bigger than yttrium. Moreover, some significant discrepancies appear in the published values of the ionic conductivity. We have accordingly carried out a systematic study of these solid solutions in order to determine their limiting compositions ( $x$  values) and to try to pin-point the essential factors determining the ionic conductivity.

## 2. Experimental procedure

### 2.1. Synthesis of the compounds

All syntheses were carried out by conventional solid state reaction techniques; the stoichiometric quantities of  $\text{NaHCO}_3$ ,  $\text{M}_2^{\text{III}}\text{O}_3$ ,  $\text{ZrO}_2$  and  $(\text{NH}_4)_2\text{HPO}_4$  were well mixed, ground and the mixture was very progressively heated in platinum crucibles up to a final temperature of 850-1150°C (depending of the composition). This temperature was maintained for 2 to 3 days with intervening mixing and grinding, until no change was observed in the X-ray powder diagram.

The weight loss was determined and was found to be in agreement with the calculated loss.

### 2.2. X-ray diffraction

The purity of all samples was checked by X-ray diffraction (CGR diffractometer,  $\text{CoK}\alpha$  radiation,  $\lambda = 0.17902$  nm).

### 2.3. Infrared spectroscopy

The spectra were recorded down to 300  $\text{cm}^{-1}$  with a Beckman 4250 spectrometer, by the conventional pressed-disc technique (KBr or NaCl discs).

### 2.4. Raman spectroscopy

The Raman spectra were recorded with a Coderg PHO double monochromator, equipped with a spectrophysics  $\text{Ar}^+$  laser. Typical conditions are 200 mW on the 514.5 nm green line, and a spectral slit width of about 3  $\text{cm}^{-1}$ .

### 2.5. Ionic conductivity

The powdered samples were cold-pressed into discs (diameter 18 mm, thickness about 1.2 mm) which were then progressively heated to the synthesis temperature. Silver paint was applied to the faces and the ohmic conductivity was determined using the complex impedances method with a Hewlett-Packard 4129A impedancemeter. The measurements are carried out in the frequency range 10 Hz to 10 MHz and in the temperature range 300 to 600 K. More details about this technique and its accuracy have been given previously [18].

## 3. Structural data

The structure of several  $\text{Na}_{1+x}\text{M}_x^{\text{III}}\text{Zr}_{2-x}(\text{PO}_4)_3$  compositions has already been described [1, 7, 9, 11, 12, 19]; they have the structure of  $\text{NaZr}_2(\text{PO}_4)_3$  (space group  $\text{D}_{3d}^6\text{-R}\bar{3}\text{c}$ ,  $Z = 6$ ) or, in some cases, ( $\text{M}^{\text{III}}$  = chromium, iron, scandium and  $x = 2$ ), they derive from this structure by a small monoclinic distortion [7, 8, 9, 11, 12, 19]. In this structure, infinite rows  $\text{O}_3\text{Zr}(\text{M}^{\text{III}})\text{O}_3\text{NaO}_3\text{Zr}(\text{M}^{\text{III}})\text{O}_3$  parallel to the  $c$ -axis are connected by  $\text{PO}_4$  groups (Fig. 1). In the parent compound  $\text{NaZr}_2(\text{PO}_4)_3$ , the  $\text{Na}^+$  cations are located inside the rows, on  $\text{M}_1$  stable sites. Three additional

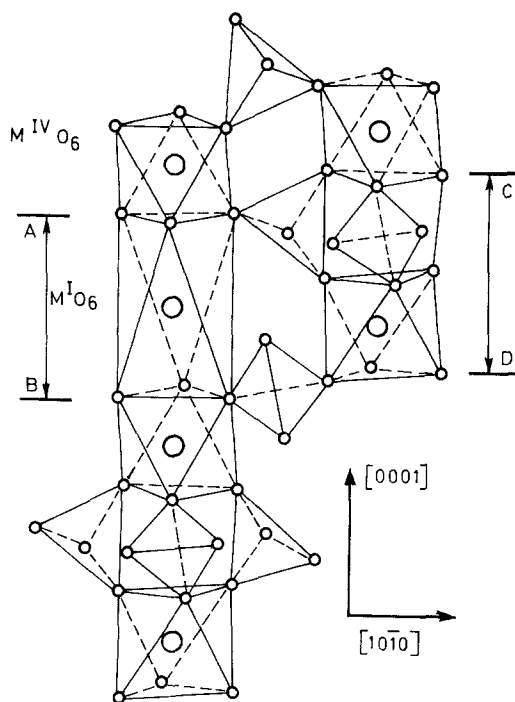


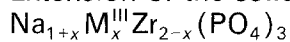
Figure 1 Part of the structure, showing the columns of  $M^I O_6$ ,  $ZrO_6$  (or  $M^{III} O_6$ ) and  $PO_4$  polyhedra, and their interconnection by  $PO_4$  tetrahedra (according to [22]).

irregular  $M_2$  sites are available between the columns and may accommodate additional  $Na^+$  cations. They are characterized by a shallow potential well and a fairly good mobility of the  $Na^+$  ions, thus leading to an important increase of the ionic conductivity [15–17].

The compounds  $Na_3 M_2^{III} (PO_4)_3$  ( $M =$  chromium, iron, scandium) are monoclinic, but the deviation from hexagonal symmetry is very small, and they exhibit, between 50 and 200°C, two phase transitions  $\alpha \rightarrow \beta$  and  $\beta \rightarrow \gamma$  eventually leading to a true hexagonal cell, isotypic with  $NaZr_2(PO_4)_3$ . These transitions are characterized by an increased disorder of the  $Na^+$  cation distribution, and an increase of the ionic conductivity. In the case of the scandium compound the importance of the monoclinic distortion and the transition temperature seems to depend on the synthesis method [14].

## 4. Results

### 4.1. Extension of the solid solutions



#### 4.1.1. $M =$ chromium, iron, scandium

Our results are in agreement with the numerous literature data showing the existence of a continuous series of solid solutions ( $0 \leq x \leq 2$ ) and a small monoclinic distortion for  $x = 2$ .

#### 4.1.2. $M =$ yttrium

We found a limited series of solid solutions, with  $x_{max}$  lying between 1.6 and 1.75, again in agreement with literature data [15].

#### 4.1.3. $M =$ dysprosium, erbium

Introducing increasing quantities of dysprosium (or erbium) brought about an increase of the  $d$  values of the X-ray powder diagram, thus showing

that we have obtained a solid solution  $Na_{1+x} Dy$  (or  $Er$ ) $_x Zr_{2-x} (PO_4)_3$ . However, we never obtained a pure, single phase: even for small  $x$  values ( $x = 0.25$ ), a small quantity of  $Dy(Er)PO_4$  was always present in the system.

#### 4.1.4. $M =$ europium, gadolinium

There was no evidence for the formation of a solid solution. The X-ray powder diagrams point to the formation of a mixture of  $NaZr_2(PO_4)_3$  and unidentified phase(s).

#### 4.1.5. $M =$ ytterbium

We found a limiting composition for  $x$  between 1.75 and 1.9 (the presence of a small quantity of a second phase for  $x = 1.9$ ), compared to  $x_{max} = 1.9$ , according to Delmas *et al.* [16, 17].

#### 4.1.6. $M =$ aluminium, gallium

Pure solid solutions were obtained for  $x$  values up to 1.25. For  $x \geq 1.50$ , early melting of the starting mixture occurred at about 750°C and no single phase was obtained. The end composition  $Na_3 Al$  (or  $Ga$ ) $_2 (PO_4)_3$  easily gave a glass which, by devitrification, gave a mixture of  $Al(Ga)PO_4$  and unidentified phases.

#### 4.1.7. $M =$ indium

According to Delmas *et al.* [17], there is a limited series of solid solutions with  $x_{max} = 1.85$ . However, we were able to prepare the pure end member ( $x = 2$ )  $Na_3 In_2 (PO_4)_3$ . All the peaks of the X-ray powder diagram (Table I) are satisfactorily accounted for by a Nasicon-like hexagonal cell with  $a = 0.8966(1)$  and  $c = 2.2104(4)$  nm:  $d_{obs} = 3.58$  g cm $^{-3}$ ,  $d_{calc} = 3.78$  g cm $^{-3}$  for  $Z = 6$ . The small standard deviation on the cell parameters, the good agreement between observed and calculated  $d$  values, and also the fact that no phase transition can be detected by differential thermal analysis and conductivity measurement, may be noticed. This suggests that, contrary to other  $Na_3 M_2^{III} (PO_4)_3$  compounds (which are only pseudo-hexagonal, but in fact monoclinic at room temperature),  $Na_3 In_2 (PO_4)_3$  is really hexagonal.

TABLE I Indexed X-ray powder diagram of  $Na_3 In_2 (PO_4)_3$

$hkl$	$d_{obs}$ (nm)	$d_{calc}$ (nm)	$I$
012	0.636	0.635	15
104	0.4498	0.4502	85
113	0.3829	0.3830	35
024	0.3176	0.3177	45
211	0.2908	0.2909	10
116	0.2846	0.2846	100
300	0.2587	0.2588	80
220	0.22425	0.22415	5
131	0.21437	0.21434	5
306	0.21173	0.21178	10
134	0.20071	0.20066	30
226	0.19148	0.19149	35
0012	0.18424	0.18420	5
137	0.17788	0.17792	5
2110	0.17655	0.17656	20
410	0.16946	0.16944	45
416	0.15395	0.15394	20
3012	0.15006	0.15008	5
330	0.14944	0.14943	10

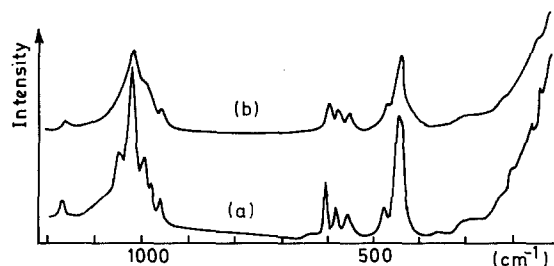


Figure 2 Raman spectra of  $\text{Na}_3\text{In}_2(\text{PO}_4)_3$ : (a) laser power = 100 mW; (b) laser power = 300 mW.

However, the Raman spectra raised some question about this conclusion. The spectrum obtained with a 100 mW laser power exhibited in the 1100 to 900  $\text{cm}^{-1}$  region a fine structure which became much more diffuse if a laser power of 300 mW was used (Fig. 2). The same result was obtained by heating the sample at about 50°C. The transformation was reversible because the fine structure was recovered after returning to room temperature and at a moderate laser power.

These results suggest a reversible order-disorder transition and are very similar to those already evinced in the case of  $\text{Na}_3\text{Fe}_2(\text{PO}_4)_3$  [20] and  $\text{Na}_3\text{Sc}_2(\text{PO}_4)_3$ . It may be recalled that, for these compounds, the  $\alpha$ -phase (stable at room temperature) is only pseudo-hexagonal, with a small monoclinic distortion. If this is also true for the indium compound, our very good hexagonal indexing suggests that the monoclinic distortion is very small.

An additional complication occurs in the infrared spectra (Fig. 3). The fine structure observed at room

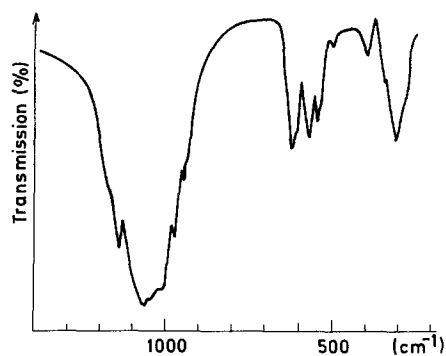


Figure 3 Infrared spectrum of  $\text{Na}_3\text{In}_2(\text{PO}_4)_3$ .

temperature does not disappear before 200°C; at higher temperatures, the spectrum is modified, but the transformation is not reversible, as if it was due to some interaction with the NaCl support. Additional work is in progress to try to understand this behaviour.

#### 4.2. Compositional range of the monoclinic distortion

Delmas *et al.* [16] have shown that, for the system  $\text{Na}_{1+x}\text{Cr}_x\text{Zr}_{2-x}(\text{PO}_4)_3$ , the monoclinic distortion observed for  $x = 2$  (i.e. the pure end member  $\text{Na}_3\text{Cr}_2(\text{PO}_4)_3$ ) disappears very rapidly when  $x$  decreases; the solid solution corresponding to  $x = 1.95$  is strictly hexagonal at room temperature. We have considered the similar iron compound  $\text{Na}_3\text{Fe}_2(\text{PO}_4)_3$  and determined (by differential thermal analysis and infrared spectroscopy) the  $\alpha \rightarrow \beta$  transition temperature as a function of various isomorphous replacements.

TABLE II  $\text{Na}_{1+x}\text{M}^{\text{III}}\text{Zr}_{2-x}(\text{PO}_4)_3$  systems

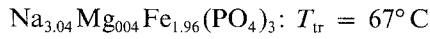
x	M	a (nm)	c (nm)	Conductivity ( $\Omega^{-1} \text{cm}^{-1}$ )		Activation energy, (kJ mol $^{-1}$ )
				$\sigma_{600\text{K}}$	$\sigma_{400\text{K}}$	
0.0	–	0.8801(1)	2.2752(5)	$7.5 \times 10^{-5}$	$1.2 \times 10^{-6}$	45.5
0.5	Al	0.8799(1)	2.2728(3)	$6.7 \times 10^{-4}$	$5.7 \times 10^{-6}$	52
0.5	Cr	0.8738(2)	2.2465(11)	$4.1 \times 10^{-4}$	$1.0 \times 10^{-5}$	41
0.5	Ga	0.8780(1)	2.2751(4)	$3.4 \times 10^{-4}$	$3.4 \times 10^{-6}$	50
0.5	In	0.8828(3)	2.2640(11)	$1.9 \times 10^{-3}$	$2.9 \times 10^{-5}$	46
0.5	Sc	0.8841(1)	2.2674(6)	$2.3 \times 10^{-3}$	$5.8 \times 10^{-5}$	41
0.5	Y	0.8878(2)	2.2776(12)	$1.4 \times 10^{-3}$	$5.6 \times 10^{-5}$	36.5
0.5	Yb	0.8884(1)	2.2796(5)	$1.2 \times 10^{-3}$	$3.0 \times 10^{-5}$	41
1.0	Al	0.8768(2)	2.2682(11)	$2.3 \times 10^{-4}$	$1.2 \times 10^{-6}$	56.5
1.0	Cr	0.8724(2)	2.2279(9)	$8.5 \times 10^{-4}$	$2.5 \times 10^{-5}$	39.5
1.0	Ga	0.8781(2)	2.2707(9)	$1.9 \times 10^{-4}$	$7.8 \times 10^{-7}$	59.5
1.0	In	0.8892(1)	2.2556(4)	$1.3 \times 10^{-3}$	$6.8 \times 10^{-5}$	34
1.0	Sc	0.8863(1)	2.2562(5)	$6.0 \times 10^{-3}$	$1.9 \times 10^{-4}$	38.5
1.0	Y	0.8982(2)	2.2885(8)	$4.2 \times 10^{-3}$	$3.3 \times 10^{-5}$	52
1.0	Yb	0.8956(2)	2.2828(6)	$2.7 \times 10^{-3}$	$1.1 \times 10^{-4}$	36
1.5	Cr	0.8671(3)	2.1967(17)	$7.2 \times 10^{-3}$	$1.8 \times 10^{-4}$	41
1.5	In	0.8908(3)	2.2400(12)	$6.4 \times 10^{-3}$	$1.0 \times 10^{-4}$	45.5
1.5	Sc	0.8899(1)	2.2444(5)	$1.2 \times 10^{-2}$	$5.6 \times 10^{-4}$	34.5
1.5	Y	0.8976(2)	2.2865(6)	$2.5 \times 10^{-3}$	$4.6 \times 10^{-5}$	44
1.5	Yb	0.9036(3)	2.2763(13)	$2.4 \times 10^{-2}$	$1.9 \times 10^{-4}$	52.5
2.0	Cr	monoclinic		$7.1 \times 10^{-3}$	$2.1 \times 10^{-5}$	67.5(LT) <sup>†</sup> 46.5(HT)
2.0	Fe	monoclinic		$1.0 \times 10^{-2}$	$1.1 \times 10^{-4}$	56.5(LT) 48.5(HT)
2.0	In	0.8966(1)	2.2101(4)	$9.0 \times 10^{-4}$	$1.2 \times 10^{-5}$	47.5
2.0	Sc	monoclinic		$(5.1 \times 10^{-2})^*$	$2.6 \times 10^{-3}$	49(LT) 34(HT)

\* Extrapolated value.

<sup>†</sup> LT = low temperature, HT = high temperature.

In the  $\text{Na}_{1+x}\text{Fe}_x\text{Zr}_{2-x}(\text{PO}_4)_3$  solid solutions, the transition temperature, which is  $96^\circ\text{C}$  for  $x = 2$ , drops to  $82^\circ\text{C}$  for  $x = 1.99$ , to  $68^\circ\text{C}$  for  $x = 1.98$  and is no longer observed for  $x = 1.95$ . A similar behaviour is observed if zirconium is replaced by hafnium, titanium or tin.

More complex substitutions lead also to a lowering of the transition temperature, e.g.



This is also true for solid solutions  $\text{Na}_3\text{Fe}_2(\text{AsO}_4)_x(\text{PO}_4)_{3-x}$  (where the number of  $\text{Na}^+$  ions remains constant) with a transition temperature of  $78^\circ\text{C}$  for  $x = 0.075$  and  $54^\circ\text{C}$  for  $x = 0.15$ . No transition is observed for  $x = 0.225$ . Thus, the transition temperature is lowered, whatever the type of substitution. This is possibly related to the fact that the  $\alpha \rightarrow \beta$  transition is of the order  $\rightarrow$  disorder type; any kind of substitution introduces some disorder which possibly promotes the transition.

### 4.3. Ionic conductivity

The results are presented in a Table II and Figs. 4 to 7. They point to an Arrhenius-like equation,  $\sigma T = Ae^{-E_a/RT}$ . The discontinuities observed for  $x = 2$  (Fig. 7) correspond to the  $\alpha \rightarrow \beta$  phase transition, in which the disordering of the  $\text{Na}^+$  cations is associated with a sharp increase of the ionic conductivity. The second  $\beta \rightarrow \gamma$  transition implies only very limited structural modifications and does not bring about significant modifications in the  $\sigma$ - $T$  relationship. Our results show clearly the influence of  $\text{M}^{\text{III}}$  on the conductivity: for a given value of  $x$ , the conductivity is generally the best for the scandium-containing phases, whereas it is worst for the aluminium and gallium compounds. These differences are only

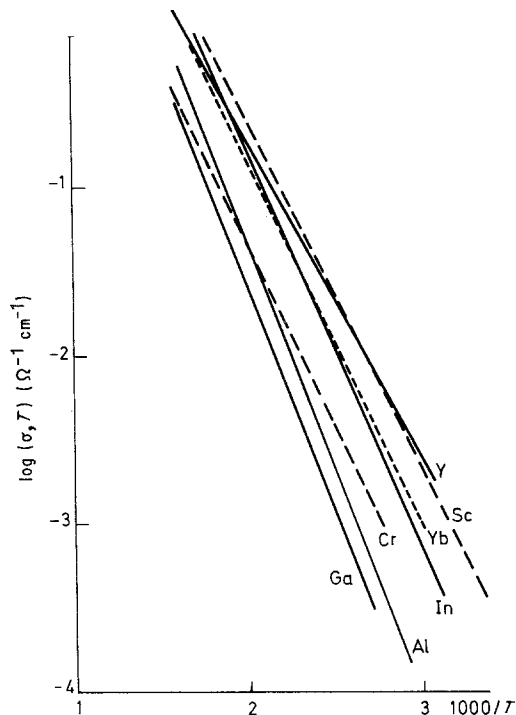


Figure 4 Ionic conductivity,  $\sigma$ , of  $\text{Na}_{1.5}\text{M}_{0.5}\text{Zr}_{1.5}(\text{PO}_4)_3$  solid solutions, as a function of  $1/T$ .

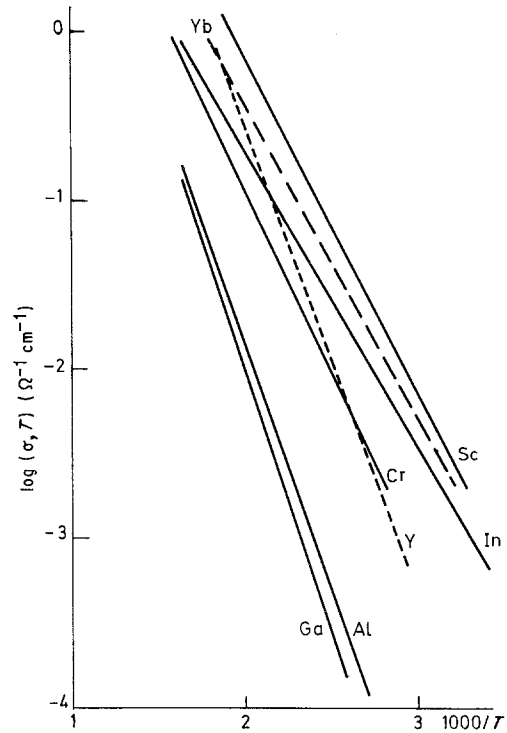


Figure 5 Ionic conductivity,  $\sigma$ , of  $\text{Na}_{2.0}\text{M}_{1.0}\text{Zr}_{1.0}(\text{PO}_4)_3$  solid solutions, as a function of  $1/T$ .

moderate for  $x = 0.5$  (Fig. 4) but much stronger for  $x = 1$  (Fig. 5).

However, the conductivity does not necessarily increase with the  $x$  value; this is true for some cations such as chromium or scandium; but for others (aluminium, gallium, indium, yttrium, ytterbium) a maximum value of conductivity is found for some intermediate value of  $x$ , this latter depending of the nature of  $\text{M}^{\text{III}}$  ([15-17] and Table II).

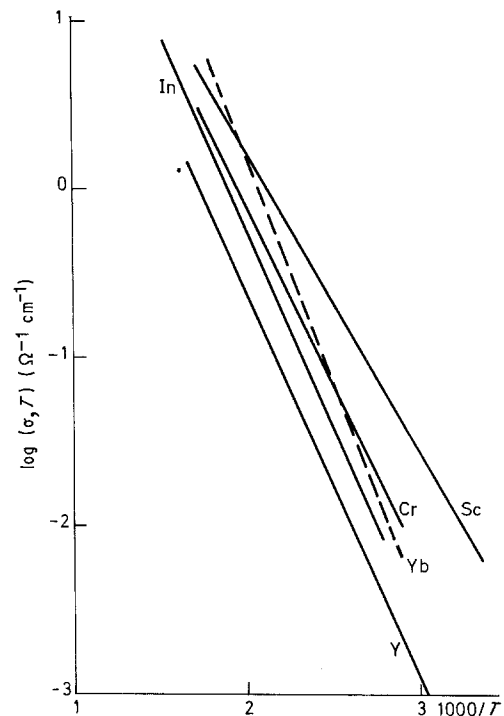


Figure 6 Ionic conductivity,  $\sigma$ , of  $\text{Na}_{2.5}\text{M}_{1.5}\text{Zr}_{0.5}(\text{PO}_4)_3$  solid solutions, as a function of  $1/T$ .

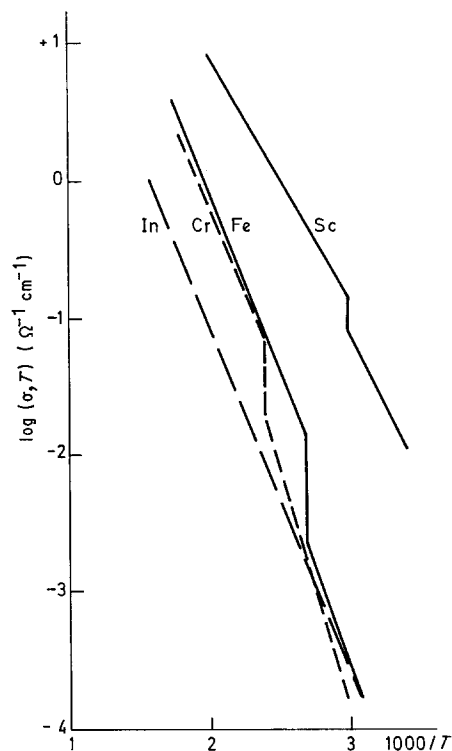


Figure 7 Ionic conductivity,  $\sigma$ , of  $\text{Na}_3\text{M}_2^{III}(\text{PO}_4)_3$  compounds, as a function of  $1/T$ .

## 5. Discussion

### 5.1. Preliminary remark

We have previously discussed [18] the reliability of the complex impedances technique as applied to sintered ceramics and we have found the different sources of errors, including the sample preparation which may affect the results. It appears from this discussion that, although acceptable, some degree of non-reproducibility is unavoidable. This should be kept in mind in the discussion, particularly when comparing the results presented by different authors.

### 5.2. Influence of the ionic radius of $\text{M}^{III}$ on the formation of solid solutions

If we take the ionic radii proposed by Shannon [21] for an octahedral coordination, it seems that the limiting ionic radius for the formation of definite solid solutions lies between 0.0900 nm ( $\text{Y}^{3+}$ ) and 0.0938 nm ( $\text{Gd}^{3+}$ ). Two comments can be made about the  $\text{Y}^{3+}$  and  $\text{Yb}^{3+}$ -containing solid solutions.

First, the maximum amount of substitution ( $x_{\text{max}}$ ) is greater for ytterbium than for yttrium, in accordance with the smaller ionic radius of  $\text{Yb}^{3+}$  (0.0868 nm).

Second, for an amount of substitution not far from  $x_{\text{max}}$ , these solid solutions are apparently metastable; after being kept for several weeks in a desiccator (which eliminates any alteration by humidity), they exhibit very significant modifications of their X-ray powder diagram. It is worth mentioning that these modifications are more important for yttrium than for ytterbium-containing phases; they do not occur for smaller trivalent cations.

This may be tentatively explained by considering that the Nasicon cell accommodates large quantities of these big cations only at relatively high temperatures (such as the synthesis temperature, about

1100°C). The shrinking of the crystal which occurs during the cooling would be responsible for the observed metastability.

### 5.3. Influence of the electronic structure of $\text{M}^{III}$ on the conductivity and on the formation of solid solutions

This point may be discussed by comparing the behaviour of the chromium- and gallium-containing phases. Both cations have very similar ionic radii (0.0615 and 0.0620 nm for  $\text{Cr}^{3+}$  and  $\text{Ga}^{3+}$ , respectively [21]) and the same electronegativity (1.6) thus suggesting other analogies in the structural properties. But the results quoted in Table II show that it is not necessarily verified: for  $x = 1$ , the unit cell parameters (and particularly the  $c$ -axis) are much greater for the gallium solid solutions, whereas its ionic conductivity is significantly smaller. Moreover, a limited quantity of gallium can be introduced in the initial Nasicon structure ( $x_{\text{max}} = 1.25$ ) whereas the introduction of chromium leads to a continuous series of solid solutions. These differences are probably related to the differences in the electronic structure of gallium (main group element) and chromium (transition element).

Some influence of the electronic structure of  $\text{M}^{IV}$  has already been found among the  $\text{NaM}_2^{IV}(\text{PO}_4)_3$  compounds: differences are observed in the vibrational pattern, even though the bands under consideration are due to vibrations of the  $\text{PO}_4^{3-}$  ions [22]; likewise, we have found that the ionic conductivity is significantly lower when  $\text{M}^{IV}$  is a main group element [23].

No definite explanation of these differences has been proposed so far, but it is perhaps useful to recall the following points:

(1) the symmetry properties of the electronic structure are not the same for the main group and for the transition elements;

(2) since we are dealing with an open structure, there is a possibility of tilting and rotating some coordinated groups, without destroying the overall hexagonal symmetry of the crystal cell (all the oxygen atoms have a site symmetry  $C_1$ );

Thus we may expect that, depending on the electronic structure of  $\text{M}^{IV}$  and  $\text{M}^{III}$  (main or transition element), the local geometry may be different. This may explain the diversity of the spectra. Moreover, this will modify the geometry of the bottlenecks and thus the ionic conductivity.

In addition to the type of electronic structure the ionic radius of  $\text{M}^{III}$  is another important factor determining the ionic conductivity. This appears clearly by comparison of the solid solutions (corresponding to  $x = 1$ ) containing either  $\text{Ga}^{3+}$  ( $r = 0.0620$  nm) or  $\text{In}^{3+}$  ( $r = 0.0800$  nm). At 400 K, the ionic conductivity of the indium compound is greater by two orders of magnitude than that of the gallium compound; at 600 K, the difference is smaller, in relation with a greater activation energy of the gallium compound. It is tempting to correlate this result with the increase in the ionic radius, and thus an expected increase of the unit cell parameters; but, in fact, we observe an increase of the  $a$  parameter, but a decrease of the  $c$  parameter (Table II).

The preceding results show that there is no simple correlation between the ionic conductivity of a solid solution and the nature and amount of the substituting cation. Some more or less empirical correlations have been presented in the literature. Thus, for the compounds  $\text{Na}_3\text{M}_2^{\text{III}}(\text{PO}_4)_3$  ( $\text{M} = \text{chromium, iron, scandium}$ ), the ionic conductivity increases with the unit cell volume [5, 12] this being explained by a widening of the migration paths. Likewise, for the  $\text{Na}_{1+x}\text{M}_x^{\text{III}}\text{Zr}_{2-x}(\text{PO}_4)_3$  solid solutions with  $\text{M} = \text{yttrium or ytterbium}$ , the highest conductivity is obtained for the highest value of the  $c$  parameter [15–17]. These correlations are certainly interesting, but it is clear that they cannot be extended to all other cationic substitutions: if this was true, the ionic conductivity of the gallium-phase would be higher than that of the chromium-phase. These difficulties are not too unexpected. Owing to the flexibility of this type of structure, we cannot predict exactly the influence of a given cation substitution on the structural parameters which determine the ionic conductivity: unit cell dimensions and local distortions, depth of the existing potential wells, diameter of the bottlenecks (which is not necessarily proportional to the unit cell dimensions).

To give a quantitative answer to these problems, a full structure determination would have to be carried out for each phase of interest. Unfortunately, this does not seem very realistic.

Finally, we shall briefly discuss the existence of breaks and discontinuities in the  $(\sigma, T)$  relationships. For  $\text{Na}_{1+x}\text{Y}_x\text{Zr}_{2-x}(\text{PO}_4)_3$  solid solutions, Nagai *et al.* [15] have observed a break of slope in the  $(\sigma, T)$  relationship indicating an increase of the activation energy. We have already discussed this phenomenon in detail and showed that this occurs when measurements are carried out at a single, too high, frequency [18].

Some discrepancies are also noticed in the case of the  $\text{Na}_3\text{M}_2^{\text{III}}(\text{PO}_4)_3$  compounds ( $\text{M} = \text{chromium, iron, scandium}$ ). According to d'Yvoire *et al.* [10], the  $\alpha \rightarrow \beta$  transition of  $\text{Na}_3\text{Cr}_2(\text{PO}_4)_3$  appears as a jump in conductivity, whereas the  $\beta \rightarrow \gamma$  transition gives only a break of slope in the  $(\sigma, T)$  relationship. This seems also to be the case for  $\text{Na}_3\text{Fe}_2(\text{PO}_4)_3$  [10] and for  $\text{Na}_3\text{Sc}_2(\text{PO}_4)_3$  [8, 13]. The small change associated with the  $\beta \rightarrow \gamma$  transition is in agreement with the fact that both phases are structurally very similar. By contrast, the results of Delmas *et al.* on  $\text{Na}_3\text{Cr}_2(\text{PO}_4)_3$  do not show the  $\alpha \rightarrow \beta$  transition [16, 17]. In our own results, the  $\alpha \rightarrow \beta$  transition always appears as a jump in conductivity (Fig. 7), but we do not see any significant break in the slope corresponding to the  $\beta \rightarrow \gamma$  transition. We can make the following comments on these negative results.

(i) A break in the slope (with a decrease of activation energy) may be due to a phase transition, but may also be explained by a difference of activation energy between the grain boundaries and the matter inside the grains [18]. This second factor is fairly frequent in ionic conductivity measurements and is

not necessarily reproducible for samples of different origins.

(ii) For the scandium compound, the  $\beta \rightarrow \gamma$  transition occurs in a temperature range where the resistivity of the sample is low, thus implying a loss of accuracy of the measurements.

(iii) For the chromium compound, the  $\alpha \rightarrow \beta$  and  $\beta \rightarrow \gamma$  transitions occur at neighbouring temperatures (138 and 166°C, respectively [10]), and the number of measurements between these temperatures is limited.

### Acknowledgements

The authors thank Professors R. Evrard and J. Depireux, Solid State Physics laboratory, for their collaboration. The Hewlett-Packard impedancemeter of this laboratory has been bought with the financial support of the Fonds National de la Recherche Scientifique.

### References

1. H. Y. P. HONG, *Mater. Res. Bull.* **11** (1976) 173.
2. J. B. GOODENOUGH, H. Y. P. HONG and J. A. KAFALAS, *ibid.* **11** (1976) 203.
3. M. PINTARD-SCRÉPEL, F. d'YVOIRE and F. RÉMY, *C.R. Acad. Sci. Paris* **286** série C (1978) 381.
4. C. DELMAS, R. OLAZCUAGA, F. CHERKAoui, R. BROCHU and G. Le FLEM, *ibid.* **287** série C (1978) 169.
5. F. d'YVOIRE, M. PINTARD-SCRÉPEL and E. BRETEY, *ibid.* **290** série C (1980) 185.
6. C. J. DELBECQ, S. A. MARSHALL and S. SUSMAN, *Solid State Ionics* **1** (1980) 145.
7. D. TRAN-QUI, J. J. CAPPONI, M. GONORAND and J. C. JOUBERT, *ibid.* **5** (1981) 305.
8. L. BOEHM, C. J. DELBECQ, E. HUTCHINSON and S. SUSMAN, *ibid.* **5** (1981) 311.
9. M. de la ROCHÈRE and F. d'YVOIRE, *ibid.* **9–10** (1983) 825.
10. *Idem*, *ibid.* **9–10** (1983) 851.
11. S. SUSMAN, C. J. DELBECQ and T. O. BRUN, *ibid.* **9–10** (1983) 839.
12. M. de la ROCHÈRE, thèse de doctorat, University Pierre et Marie Curie, Paris VI (1984).
13. S. YU. STEFANOVIČH, V. B. KALININ and A. NOGAI, *Ferroelectrics* **55** (1984) 325.
14. M. BARJ, H. PERTHUIS and Ph. COLOMBAN, *Solid State Ionics*, **11** (1983) 157.
15. M. NAGAI, S. FUJITSU and T. KANAZAWA, *J. Amer. Ceram. Soc.* **63** (1980) 476.
16. C. DELMAS, J. C. VIALA, R. OLAZCUAGA, G. Le FLEM and P. HAGENMULLER, *Mater. Res. Bull.* **16** (1981) 83.
17. *Idem*, *Solid State Ionics* **3/4** (1981) 209.
18. J. M. WINAND and J. DEPIREUX, *Europhys. Lett.*, **8** (1989) 447.
19. L. O. HAGMAN and P. KIERKEGAARD, *Acta Chem. Scand.* **22** (6) (1968) 1822.
20. P. TARTE, J. M. WINAND and A. RULMONT, *C.R. Acad. Sci. Paris* **302** série II (1986) 553.
21. R. D. SHANNON, *Acta Crystallogr.* **A32** (1976) 751.
22. P. TARTE, A. RULMONT and C. MERCKAERT-ANSAY, *Spectrochim. Acta* **42A** (1986) 1009.
23. J. M. WINAND, P. TARTE and A. RULMONT, to be published.

Received 4 May

and accepted 29 September 1989